

# Spectroscopy with a mode-locked Femtosecond Laser Frequency Comb

Vela Mbele and Elias Sideras-Haddad

School of Physics, University of the Witwatersrand, 1 Jan Smuts, Braamfontein, Johannesburg

E-mail: m.l.vela@yahoo.com

**Abstract.** We summarise high-resolution, high-precision spectroscopy experiment where caesium-133 atoms in a vapour cell are excited directly with a femtosecond laser frequency comb. In this experiment the laser beam is sent counter-propagating by the beam-splitting cube, focussed to a reasonable waist in the interaction region in the vapour cell, thereby exciting a multitude of low lying transitions allowing the measurement of transition energies and hyperfine coupling coefficients for the  $8S_{1/2}$ ,  $9S_{1/2}$  and  $7D_{3/2,5/2}$  states.

## 1. Introduction

The technology awarded the one-half of the 2005 Nobel prize for Physics involving a mode-locked femtosecond laser frequency comb (FLFC) [1] has been gaining in the range of applications over the past years. This technology originally designed to count cycles in optical clocks, now has applications extending over a vast array of research areas including spectroscopy, trace gas detection, signal processing, astrophysics and many others. The basic ideas of using repetitive pulses and mode-locked lasers for high-resolution precision spectroscopy followed soon after the development of the laser itself, in the early 1970s. Stabilization of optical frequency combs [2], in the mid to late 1990's triggered and stimulated this renewed interest and the many spectroscopic applications of mode locked laser's [3, and references therein].

The higher intensities and longer coherence lengths in lasers allowed scientists to perform experiments, that had until then only been restricted to the theoretical domain, with some of the predicted experiments that could not be performed with the lamps (see for an example earlier work in caesium [4]) that were used in earlier years of spectroscopic studies. Experiments which had, before the advent of the laser, been only restricted to theoretical predictions included Doppler-free two photon transitions [5]. The two-photon theory underlying these experiments had been predicted long before the lasers were developed [6](see also, for example, the review [7, and references therein] and the theoretical formalization that followed after the development of the laser [8]).

Precision laser atomic spectroscopy, has and continues to play an important role in fundamental physics studies [9, 10, 11, 12, 13, 14, 15, 16]. On the one hand, caesium is an important, and continues to be, a test-bed for fundamental studies and atomic theory [9]. Hyperfine interactions are sensitive to the details of nuclear structure, electron correlations, relativistic and core polarisation effects. The correlational effects come about because of the degree to which the P – D effects mix into S – S parity violation amplitudes. Generally, experimental considerations usually restrict high precision work to S and P states [13, 16, 17], while measurements in the D states still remain a challenge because of correlational effects [18] and hence a need for more measurements in the D states [19], answered in part in the work presented here.

There is a likelihood that in the passing time, these applications may be taken over by the compact monolithic micro-resonator generated frequency combs [20, 21], there is, however, no doubt that mode-locked FLFC will continue growing their range of applicability over the next few decades.

## 2. The femtosecond frequency comb

The femtosecond laser frequency comb used in these measurements is based on the Kerr-lens mode-locked [22] titanium doped sapphire (Ti:Sa) crystal laser. The octave-spanning nature of this laser, with radiation ranging from 530 nm to well above 1200 nm, aids in the self-referencing [2]. The frequency mode structure of the femtosecond laser comb can be understood from mode-locking which is dependent on time/frequency domain structure of mode-locked lasers. Generally, any single pulse will have a spectrum that is the Fourier transform of its envelope function and centered at the optical frequency of its carrier and for any pulse shape, the frequency width of the spectrum will be inversely proportional to the temporal width of the envelope. On the other hand, for pulses separated by a fixed interval, the spectrum is obtained by a Fourier series expansion, yielding a comb of regularly spaced frequencies, where the comb spacing is inversely proportional to time between pulses, and rigidly shifted in the event of there being a carrier envelope phase. The spacing between the comb modes is the repetition rate,  $f_{\text{rep}}$  and the carrier envelope phase dependent shift is the offset frequency,  $f_0$ , such that the optical frequency of the  $n$ -th of those comb modes is

$$\nu_n = n f_{\text{rep}} + f_0, \quad (1)$$

where  $n$  ranges from 250 000 to 570 000. The successive slip of the phase with each pulse,  $\Delta\phi$ , the repetition rate  $f_{\text{rep}}$  and the offset frequency,  $f_0$ , are related by

$$\Delta\phi = 2\pi(f_0/f_{\text{rep}}). \quad (2)$$

It is Equation 1 that provides the optical frequency comb with the “gearbox” [21] capability which enables the reliable and accurate means of counting optical cycles on the femtosecond ( $10^{-15}$  s) time scale, the single most important character in the realization of optical clocks. The accuracy of such clocks is now measured to the 18th digit [23], exceeding the performance of their microwave counterparts by more than an order of magnitude. This development involves the measurement of the energy structure of atoms at an unprecedented level, allowing some of the most precise laboratory tests of the physics governing these systems.

With the low noise microwave standard as a reference the frequency of each element of the comb can be determined absolutely with a fractional uncertainty at or below  $\sim 2 \times 10^{-13}/\sqrt{\tau}$  where  $\tau$  is the averaging in seconds or longer. Optical clocks are fast getting to their quality factor,  $\Delta f/f$ , limit [23] and the use of an optical reference would provide  $\sim 1$  Hz optical resolution and fractional uncertainty of a few parts in  $\sim 10^{17}$  range, the microwave reference is sufficient for these experiments. For the type of spectroscopy experiments we report in this work the atomic reference provided by the global positioning system (GPS) or the commercially available beam clocks would be more than adequate. Stated alternatively, the linewidth of the comb modes  $\sim 100$  kHz with the maser reference and could be a few Hz if the laser comb were referenced to optical clock. This study also serves to re-affirm the need of improved references and hence all laboratories with capabilities should look into developing their own optical standards.

## 3. The caesium experiment

The experimental set-up block diagram of the caesium experiment is shown in Fig. 1. Radiation from the laser is sent to a caesium vapour cell via two beam-split routes. In each route the laser radiation is filtered, by the optical bandpass filters marked F1 and F2, to isolate individual states and to eliminate excitation by Doppler broadened co-propagating photons, otherwise without the filters the collected spectrum is complicated, as can be seen in Fig. 3, and introduction of the filters to isolate on eof the states results in the spectrum

shown in Fig. 4. The excitation pathways are shown Figure 2. Fluorescence collected from the  $7P_{1/2, 3/2}$  states is detected by a photomultiplier tube placed next to the vapour cell. We used the bandpass filter marked F3 is to isolate this decay while also eliminating the background scattering.

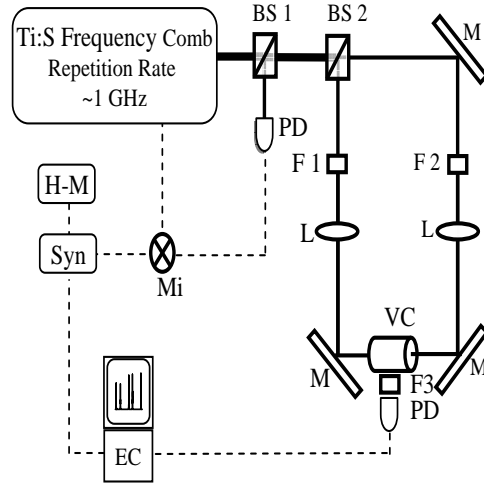


**Figure 1:** Block diagram of the Cs spectrometre using the femtosecond frequency comb and a Cs vapor cell (VC). The other components are: BS, beamsplitter; M, mirror; F1, F2, F3 bandpass filters; L, lens; PD, photodetector; Mi, Mixer; SYN, frequency synthesizer; H-M, hydrogen maser and EC, denotes the data collection and experimental control computer.

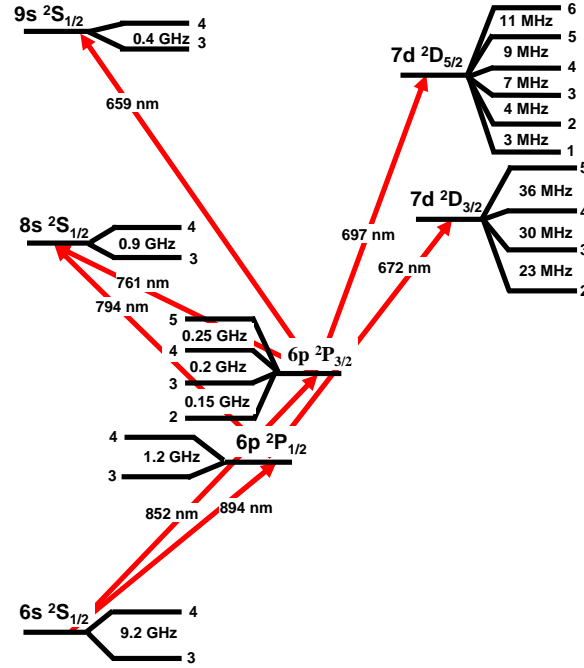


**Figure 2:** The excitation pathways to the low lying positive parity energy-levels in Cs excited by the radiation within the mode-locked laser radiation bandwidth. The two-photon is resonant with the real intermediate state and subsequently excited to the final state.

The filters are shown in Table 1, where F1 is the filter used in either the D1 or D2 transitions in the one arm and F2 the complimentary excitation to the higher state in other. The laser spectrum had sufficient light intensities to allow access of the  $8S$  state through both of the  $6P_{1/2,3/2}$  states as the intermediary state. We could only access the  $9S_{1/2}$  state through the  $6P_{3/2}$  because of lack of sufficient light intensities in the complimentary radiation so as to excite this state through the  $6P_{1/2}$  state. In anyway, our ability to measure the  $8S_{1/2}$  state through both of the intermediate states allowed us to use the  $8S_{1/2}$  state to check for repeatability in our measurements by quantifying the agreement in the absolute frequency and the hyperfine coupling constant measurements attained through the two different excitation pathways. We found very good agreement between the two sets of measurements. This agreement also augured well for the validity of our method of analysis.

The data for the  $7D_{3/2}$  was only collected through the D1 transition, because the manifold structures of both the  $7D_{3/2}$  and  $6P_{3/2}$  states resulted in a complicated spectrum. Another complication we had was that the fine-structure splitting between the  $7D_{5/2}$  and  $7D_{3/2}$  states is so small such that it was impossible to selectively excite both of the states through the  $6P_{3/2}$  state, as such the  $7D_{3/2}$  state was only excited through the D1 transition, and the  $7D_{5/2}$  through the D2 transition. Furthermore, selection rule considerations do not allow electric dipole transitions through the  $6P_{1/2}$  to  $7D_{5/2}$ , because that would have meant  $\Delta J = 5/2 - 1/2 = 2$  for the electric dipole transition. We still had a residual  $7D_{3/2}$  detected, together with the  $7D_{5/2}$ . The  $7D_{3/2}$  is accessible through both routes. This

was because the wavelengths connecting  $6P_{3/2}$  to the two  $7D_{3/2}$  and  $7D_{5/2}$  states are 698 nm and 697 nm, respectively. This made it impossible to completely separate the  $7D_{3/2}$  contribution from the  $7D_{5/2}$  using the bandpass filters available to us. However, the matrix elements for the  $6P_{3/2} \rightarrow 7D_{5/2}$  were far stronger than the corresponding  $6P_{3/2} \rightarrow 7D_{3/2}$  matrix elements. This fact coupled with that 698 nm was on the edge of the bandpass filter we used to excite the complementary transition allowed us to extract  $6P_{3/2} \rightarrow 7D_{5/2}$ .

**Table 1:** Optical filters and combinations thereof used as F1 and F2 in Fig. 1. Wavelengths are in nanometers, followed by transmission bandwidth (nm), l.p. indicates long-pass and s.p. short-pass edge filters.

Final	Intermediate	Filter 1	Filter 2
$8S_{1/2}$	$6P_{1/2}$	890 (10)	755(40)/715 l.p.
$8S_{1/2}$	$6P_{3/2}$	850 (10)	800 s.p./780 l.p.
$9S_{1/2}$	$6P_{3/2}$	850 (10)	657.9 (10)
$7D_{3/2}$	$6P_{1/2}$	890 (10)	670 (30)
$7D_{5/2}$	$6P_{3/2}$	850 (10)	700 (25)

The probability that the atom will make a transition is therefore the second-order time-dependent perturbation theory given by

$$P(6S_{\frac{1}{2}} : n''L''_{J''}) \propto \frac{1}{2F+1} \frac{I_1 I_2}{\left[ \omega_{6S_{\frac{1}{2}}F:n''L''_{J''}F''} - (\omega_1 + \vec{k}_1 \cdot \vec{v}) - (\omega_2 + \vec{k}_2 \cdot \vec{v}) \right]^2 + \left( \frac{\gamma_{n''L''}}{2} \right)^2} \times \sum_{M_F, M'_F} \left| \sum_{F', M''_F} \frac{\langle n''L''_{J''}F''M''_F | \hat{e}_2 \cdot \vec{d} | 6P'_{J'}F'M'_F \rangle \langle 6P'_{J'}F'M'_F | \hat{e}_1 \cdot \vec{d} | 6S_{\frac{1}{2}}FM_F \rangle}{\omega_{6S_{\frac{1}{2}}F:6P'_{J'}F'} - (\omega_1 + \vec{k}_1 \cdot \vec{v}) - i\gamma_{6P_{J'}}} \right|^2. \quad (3)$$

In Equation 3,  $\vec{v}$  is the atomic velocity,  $\vec{d}$  the electric dipole operator,  $M_F$ ,  $M'_F$  and  $M''_F$  are the projections of  $F$ ,  $F'$  and  $F''$  along the quantization axis,  $\hat{e}_1$  is the unit vector in the polarisation direction of the beam with wave vector  $\vec{k}_1$  and  $\hat{e}_2$  is the same for  $\vec{k}_2$ . We use Equation 3 to reproduce the spectra, with the resulting spectra being used in the extraction of the absolute frequencies and the hyperfine coupling coefficients, by fitting the peak frequencies from the experimental and the calculated spectra. We designate the peak centers in the repetition rate frequencies of the experimental spectra,  $f^{\text{expt}}$ , and the theoretical spectra,  $f^{\text{calc}}$ . For each peak we then evaluate the  $\chi^2$  function, as a normalized difference between the calculated interpolating function and the experimental data,

$$\chi^2(\Delta\nu_{6S-n''L''_{J''}}, \Delta A_{n''L''}, \Delta B_{n''L''}) = \sum_i \left( \frac{f_i^{\text{expt}} - f_i^{\text{calc}}(\Delta\nu_{6S-n''L''_{J''}}, \Delta A_{n''L''}, \Delta B_{n''L''})}{\sigma_i^{\text{expt}}} \right)^2, \quad (4)$$

Table 2 shows all the frequencies calculated and inferred from these measurements.

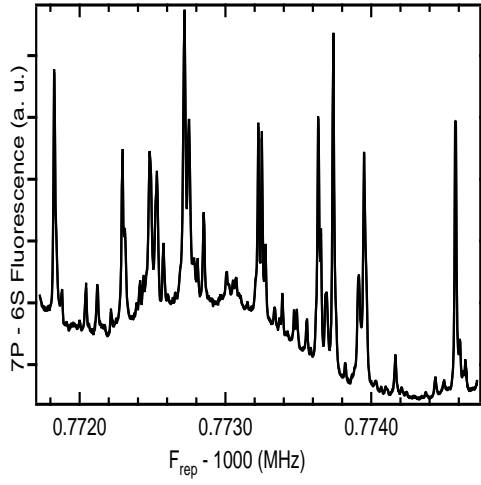


**Figure 3:** Caesium fluorescence from  $7P_{1/2,3/2} \rightarrow 6S_{1/2}$  decay. To collect the spectrum the laser cavity is scanned without the filters (F1 and F2, Fig. 1) which we use to restrict the laser's spectral bandwidth.

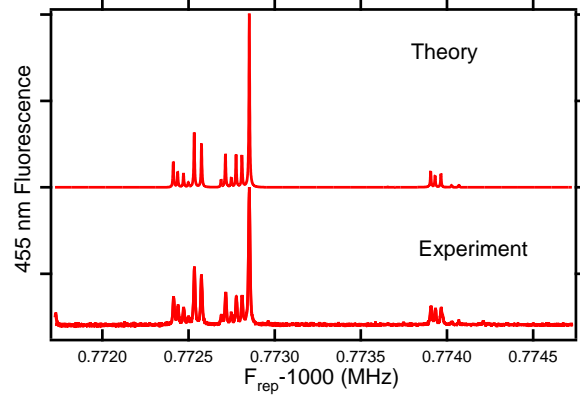


**Figure 4:** Spectrum of the  $6S_{1/2} - 7D_{3/2}$  transition via  $6P_{1/2}$  intermediate state. The lower of the two traces is the experimental data and the other the modeled spectrum. The plot shows the fluorescence intensity from the  $7P$  to  $6S$  decay as a function of the laser repetition rate,  $f_{\text{rep}}$ .

**Table 2:** The single photon transition frequencies,  $\nu_{6S_{1/2} \rightarrow n''L''_{j''}}$ , hyperfine coupling coefficients,  $A_{n''L''_{j''}}$  and  $B_{n''L''_{j''}}$ , with the complementary transition frequencies,  $\nu_{6P_{1/2} \rightarrow n''L''_{j''}}$  and  $\nu_{6P_{3/2} \rightarrow n''L''_{j''}}$  and  $\nu_{FF''}$  measured in this work.

Parameter	$8S_{1/2}$	$9S_{1/2}$	$7D_{3/2}$	$7D_{5/2}$
$\nu_{6S_{1/2} \rightarrow n''L''_{j''}}$	729 009 798.86(15)	806 761 363.14(10)	780 894 762.250(64)	781 522 153.68(16)
$A_{n''L''_{j''}}$	219.133(75)	109.932(50)	+7.386(18)	-1.717(15)
$B_{n''L''_{j''}}$			-0.182(163)	-0.182(517)
$\nu_{6P_{1/2} \rightarrow n''L''_{j''}}$	393 893 750.11(15)	471 645 314.63(10)	445 778 713.502(64)	446 406 104.93(16)
$\nu_{6P_{3/2} \rightarrow n''L''_{j''}}$	377 284 080.39(15)	455 035 644.91(10)	429 169 043.778(64)	429 796 435.21(16)
$\nu_{31}$				781 527 343.75(36)
$\nu_{32}$			780 899 883.152(163)	781 527 340.37(25)
$\nu_{33}$	729 014 476.67(22)	806 766 286.89(15)	780 899 905.440(97)	781 527 335.28(19)
$\nu_{34}$	729 015 353.20(20)	806 766 726.62(13)	780 899 935.036(99)	781 527 328.45(23)
$\nu_{35}$			780 899 971.836(121)	781 527 319.86(22)
$\nu_{42}$			780 890 690.521(163)	781 518 147.74(25)
$\nu_{43}$	729 005 284.03(22)	806 757 094.26(15)	780 890 712.809(97)	781 518 142.65(19)
$\nu_{44}$	729 006 160.57(20)	806 757 533.98(13)	780 890 742.405(100)	781 518 135.82(23)
$\nu_{45}$			780 890 779.205(121)	781 518 127.23(22)
$\nu_{46}$				781 518 116.83(24)

## References

- [1] John L. Hall. *Rev. Mod. Phys.*, 78(4):1279–1295, 2006; Theodor W. Hänsch. *Rev. Mod. Phys.*, 78(4):1297–1309, 2006.
- [2] D. J. Jones, S. A. Diddams, J. K. Ranka, A. Stentz, R. S. Windeler, J. L. Hall, and S. T. Cundiff. *Science*, 288:635–9, 2000.
- [3] M. C. Stowe, M. J. Thorpe, A. Péer, J. Ye, J. E. Stalnaker, V. Gerginov, and S. A. Diddams. *Adv. At. Mol. Opt. Phys.*, 55:1–60, 2008; S. A. Diddams. *J. Opt. Soc. Am. B*, 27:B51 – B62, 2010.
- [4] H. Kleiman and K. W. Meissner. *TECHNICAL REPORT No. 1.*, pages 1–29, 1 October 1959; H. Kleiman. *J. Opt. Soc. Am.*, 52(4):441–447, 1962.
- [5] F. Biraben, B. Cagnac, and G. Grynberg. *Phys. Rev. Lett.*, 32:643–645, 1974; F. Biraben, B. Cagnac, and G. Grynberg. *Phys. Lett. A*, 48:469, 1974; M.D. Levenson and N. Bloembergen. *Phys. Rev. Lett.*, 32:645, 1974; T.W. Hänsch, K. Harvey, and G. Meisel. *Opt. Comm.*, 11:50, 1974.

- [6] M. Göppert-Mayer. *Annalen der Physik*, 9(2):272–294, 1931.
- [7] N. Bloembergen. *Rev. Mod. Phys.*, 54:685–695, 1982.
- [8] L. S. Vasilenko, V. P. Chebotaev, and A.V. Shishaev. *JETP Lett.*, 12:113, 1970.
- [9] J. Guena, M. Lintz, and M-A. Bouchiat. *J. Opt. Soc. Am. B*, 22:21 – 28, 2005; C. S. Wood, S. C. Bennett, D. Cho, B. P. Masterson, J. L. Roberts, C. E. Tanner, and C. E. Wieman. *Science*, 275:1759–1763, 1997.
- [10] S. C. Bennett and C. E. Wieman. *Phys. Rev. Lett.*, 82:2484–7, 1999.
- [11] S. A. Murthy, D. Krause, Z. L. Li, and L. R. Hunter. *Phys. Rev. Lett.*, 63:965, 1989; H. S. Nataraj, B. K. Sahoo, B. P. Das, and D. Murkherjee. *Phys. Rev. Lett.*, 101:033002, 2008.
- [12] A. Wicht, J. M. Hensley, E. Sarajlic, and S. Chu. *Phys. Scr.*, T102:82–88, 2002; G. Gabrielse, D. D. Hanneke, T. Kinoshita, M. Nio, and B. Odom. *Phys. Rev. Lett.*, 97:030802–1–4, 2006.
- [13] V. Gerginov, K. Calkins, C. E. Tanner, J. J. MacFerran, S. A. Diddams, A. Bartels, and L. Hollberg. *Phys. Rev. A*, 73:032504–1–10, 2006.
- [14] Peter J. Mohr, Barry N. Taylor, and David B. Newell. *Rev. Mod. Phys.*, 80:633–730, 2008; Ulrich D. Jentschura, Peter J. Mohr, Joseph N. Tan, and Benedikt J. Wundt. *Phys. Rev. Lett.*, 100:160404, 2008; B. J. Wundt and U. D. Jentschura. *J. Phys. B: At. Mol. Opt. Phys.*, 343:115002, 2010.
- [15] E. Peik, B. Lipphardt, H. Schnatz, T. Schneider, Chr. Tamm, and S. G. Karshenboim. *Phys. Rev. Lett.*, 93:170801, 2004; Chr. Tamm, T. Schneider, and E. Peik. Trapped Ion Optical Frequency Standards for Laboratory Tests for Alpha-Variability. In S. G. Karshenboim and E. Peik, editors, *Lecture Notes in Physics: Astrophysics, Clocks and Fundamental Constants*, chapter 15, pages 247–261. Springer, Berlin, 2004; T. M. Fortier, N. Ashby, J. C. Bergquist, M. J. Delaney, S. A. Diddams, T. P. Heavner, L. Hollberg, W. M. Itano, S. R. Jefferts, K. Kim, et al. *Phys. Rev. Lett.*, 98:070801, 2007.
- [16] V. Gerginov, C. E. Tanner, and A. Derevianko. *Phys. Rev. Lett.*, 91:072501–1–4, 2003.
- [17] A. Kortyna, N. A. Masluk, and T. Bragdon. *Phys. Rev. A*, 74:022503–1–6, 2006; M. S. Safronova, W. R. Johnson, and A. Derevankio. *Phys. Rev. A*, 60:4476–4487, 1999; V. Gerginov, C. E. Tanner, S. A. Diddams, A. Bartels, and L. Hollberg. *Phys. Rev. A*, 70:042505–1–8, 2004.
- [18] V. A. Dzuba, V. V. Flambaum, and J. S. M. Ginges. *Phys. Rev. A*, 63:062101, 2001.
- [19] M. S. Safronova and Charles W. Clark. *Phys. Rev. A*, 69:040501, 2004.
- [20] P. Del’Haye, A. Schliesser, O. Arcizet, T. Wilken, R. Holzwarth, and T. J. Kippenberg. *Nature*, 450:1214–1217, 2007.
- [21] T. J. Kippenberg, R. Holzwarth, and S. A. Diddams. *Science*, 332:555–559, 2011.
- [22] A. Bartels. Gigahertz Femtosecond Lasers: The tools for precise optical metrology. In J. Ye and S. T. Cundiff, editors, *Femtosecond Optical Frequency Comb Technology: Principle, Operation and Application*, chapter 3, pages 78–96. Springer, New York, 2005.
- [23] W. H. Oskay, W. M. Itano, and J. C. Bergquist. *Phys. Rev. Lett.*, 94:163001, 2005; T. Rosenband, D. B. Hume, P. O. Schmidt, C. W. Chou, A. Brusch, L. Lorini, W. H. Oskay, R. E. Drullinger, T. M. Fortier, J. E. Stalnaker, et al. *Science*, 319:1808–1812, 2008.